

## Oscillatory changes in the tunneling magnetoresistance effect in semiconductor quantum-dot spin valves

K. Hamaya,<sup>1,2,\*</sup> M. Kitabatake,<sup>1</sup> K. Shibata,<sup>1</sup> M. Jung,<sup>1</sup> M. Kawamura,<sup>1</sup> S. Ishida,<sup>3</sup> T. Taniyama,<sup>4,5</sup> K. Hirakawa,<sup>1,2,6</sup> Y. Arakawa,<sup>1,2,3</sup> and T. Machida<sup>1,2,6,†</sup>

<sup>1</sup>*Institute of Industrial Science, University of Tokyo, 4-6-1 Komaba, Meguro-ku, Tokyo 153-8505, Japan*

<sup>2</sup>*Institute for Nano Quantum Information Electronics, University of Tokyo, 4-6-1 Komaba, Meguro-ku, Tokyo 153-8505, Japan*

<sup>3</sup>*Research Center for Advanced Science and Technology, University of Tokyo, 4-6-1 Komaba, Meguro-ku, Tokyo 153-8505, Japan*

<sup>4</sup>*Materials and Structures Laboratory, Tokyo Institute of Technology, 4259 Nagatsuta, Midori-ku, Yokohama 226-8503, Japan*

<sup>5</sup>*Japan Science and Technology Agency, PRESTO, 4-1-8 Honcho, Kawaguchi 332-0012, Japan*

<sup>6</sup>*Japan Science and Technology Agency, CREST, 4-1-8 Honcho, Kawaguchi 332-0012, Japan*

(Received 3 November 2007; revised manuscript received 4 December 2007; published 7 February 2008)

We experimentally study the tunneling magnetoresistance (TMR) effect as a function of bias voltage ( $V_{SD}$ ) in lateral Ni/InAs/Ni quantum-dot (QD) spin valves showing Coulomb blockade characteristics. With varying  $V_{SD}$ , the TMR value oscillates and the oscillation period corresponds to conductance changes observed in the current-voltage ( $I$ - $V_{SD}$ ) characteristics. We also find an inverse TMR effect near  $V_{SD}$  values where negative differential conductance is observed. A possible mechanism of the TMR oscillation is discussed in terms of spin accumulation on the QD and spin-dependent transport properties via excited states.

DOI: [10.1103/PhysRevB.77.081302](https://doi.org/10.1103/PhysRevB.77.081302)

PACS number(s): 85.75.-d, 73.23.Hk, 73.21.La

Spin-dependent single-electron tunneling and its related transport phenomena have been studied experimentally in micro- or nanofabricated double-barrier junctions which consist of a small metallic or molecule island and ferromagnetic electrodes (FEs).<sup>1-7</sup> In Co/Co-Al-O/Al-O/Al junctions,<sup>5</sup> Yakushiji *et al.* reported tunneling magnetoresistance (TMR) oscillations as a function of bias voltage ( $V_{SD}$ ) and an enhanced spin lifetime in Co nanoparticles, which are induced by spin accumulation due to an injection of spin-polarized electrons. Recently, Bernand-Mantel *et al.* demonstrated an inverse TMR effect through a *single* Au nanoparticle in Co/Al<sub>2</sub>O<sub>3</sub>/Au/Al<sub>2</sub>O<sub>3</sub>/Co nanojunctions.<sup>6</sup>

Up to now, lots of theoretical studies of the metallic quantum-dot (QD) spin valves (SVs) have also reported the effect of spin accumulation, which causes the spin splitting of the Fermi level in the QD, on the TMR.<sup>2,5,6,8-16</sup> These studies described that a spin accumulation with Coulomb blockade characteristics leads to an oscillatory variation in the TMR value with varying  $V_{SD}$ ,<sup>8-16</sup> and a marked splitting of the spin states in the QD can induce a sign inversion of the TMR.<sup>8,9,16</sup> In addition to these considerations, recent theories have also discussed that orbital levels in the QD can affect the spin-dependent transport properties.<sup>12,13,17-19</sup> Weymann and Barnaś predicted that the effect of the orbital levels leads to negative differential conductance (NDC) and oscillatory changes in the TMR effect in a finite- $V_{SD}$  regime.<sup>18</sup>

For semiconductor systems, we recently succeeded in the fabrication of Co/InAs/Co lateral QDSVs and observed TMR effect.<sup>20</sup> Also, an electric-field control of the TMR effect was demonstrated in Ni/InAs/Ni QDSV devices.<sup>21</sup> However, the origin of the TMR effect observed remains elusive. To exhibit the first experimental results for semiconductor QDSVs and to understand the mechanism of the TMR effect, we should study the dependence of the TMR effect on  $V_{SD}$ .<sup>5,6,8-18</sup>

In this work, we examine TMR effect as a function of  $V_{SD}$  in lateral semiconductor QDSVs—i.e., Ni/InAs/Ni devices.

We show an oscillatory variation in the TMR value with increasing  $V_{SD}$ . The oscillation period corresponds to fine conductance changes observed in current-voltage ( $I$ - $V_{SD}$ ) characteristics. Also, an inverse TMR effect is observed at  $V_{SD}$  where negative differential conductance is seen. We discuss a possible mechanism of the TMR oscillation in terms of spin accumulation on the QD and spin-dependent transport properties through excited states.

Self-assembled InAs QDs were grown on a substrate made of 170-nm-thick GaAs buffer layer/90-nm-thick AlGaAs insulating layer/ $n^+$ -GaAs(001) which is utilized as the backgate electrode. The Ni/InAs/Ni QDSV devices were fabricated by using a conventional electron-beam lithography and lift-off method, as shown in our previous reports.<sup>20,21</sup> The same fabrication process was utilized for observing the Kondo effect in Ni/InAs QD (ferromagnetic metal/QD) (Ref. 22) and Al/InAs QD (superconducting metal/QD) (Ref. 23) interfaces, so that we believe that the quality of the Ni/InAs QD interface is guaranteed for obtaining spin-related properties. A schematic diagram of our device is illustrated in Fig. 1(a). A single InAs QD is weakly coupled to two Ni electrodes that have a thickness of 40 nm and asymmetric wire shapes.<sup>20,21</sup> The size of the InAs QD is  $\sim 120$  nm, and both Ni electrodes overlap the InAs QD. Transport measurements were performed by a dc method in a dilution refrigerator at  $T \sim 50$  mK. External magnetic fields ( $B$ ) were applied parallel to the long axis of the wires. The magnetoresistance (MR) ratio (%) is defined as  $\{(I_0 - I_B)/I_B\} \times 100$ , where  $I_0$  and  $I_B$  are the tunnel currents for zero field and for a magnetic field of  $B$ , respectively.

Prior to exploring the MR features, we first measured the  $I$ - $V_{SD}$  characteristics of the device for various  $V_G$ , where  $V_G$  is the backgate voltage. The tunnel resistance was much larger than the quantum resistance of  $h/e^2 \sim 25.8$  k $\Omega$ , so that electrons tunnel sequentially through the QD. In Fig. 1(b) diamondlike changes in the differential conductance  $dI/dV_{SD}$  are observed as a function of  $V_{SD}$  and  $V_G$  for a parallel mag-

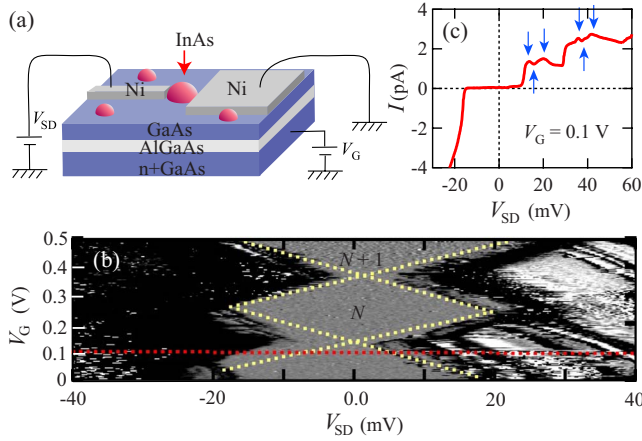


FIG. 1. (Color online) (a) A schematic diagram of our lateral quantum-dot spin-valve device. (b) A two-dimensional plot of differential conductance  $dI/dV_{SD}$  as a function of  $V_{SD}$  and  $V_G$  in parallel magnetic configuration at  $B=0.1$  T and  $T=50$  mK. (c)  $I$ - $V_{SD}$  curve measured at  $V_G=0.1$  V.

netic configuration of Ni electrodes ( $B \sim 0.1$  T). The gray region indicates the Coulomb blockade regime, and the black and white regions are the regimes of  $dI/dV_{SD} > 0$  and  $dI/dV_{SD} < 0$ , respectively. The charging energy  $E_c$  estimated from the Coulomb diamond was  $\sim 18$  meV. Although the number of electrons ( $N$ ) observed here is likely in between  $N=5$  and  $15$ , we could not assign it exactly for this device. Note that the NDC ( $dI/dV_{SD} < 0$ ) varies systematically with  $V_G$  and the NDC strips run almost parallel to a direction of the diamond edges. We also present an  $I$ - $V_{SD}$  curve at  $B \sim 0.1$  T in Fig. 1(c), measured at  $V_G=0.1$  V [the cross section of the red (dark gray) dashed curve in Fig. 1(b)]. The Coulomb staircases are identified in the positive  $V_{SD}$  regime, together with the fine structures (see arrows). The fine structures arise from the presence of the conductance strips observed in Fig. 1(b), which are inherent properties of our device. The energy spacing between the fine structures is smaller than  $E_c \sim 18$  meV. From these results, we conclude that the fine structures observed between the Coulomb staircases originate from the excited states due to the orbital energy levels  $\epsilon$  of the QD ( $E_c > \delta\epsilon$ ).<sup>12,13</sup> Furthermore, the very asymmetric  $I$ - $V_{SD}$  feature is shown about the polarity of  $V_{SD}$ , which is probably caused by the quite asymmetric tunnel barriers. With regard to this, the coupling strength between electrons in the InAs QD and in the Ni electrodes can also be deduced to be asymmetric.

Next, we examine MR features for various  $V_{SD}$  at  $V_G=0.1$  V. The representative MR curves are shown in Fig. 2, in which the red (dark gray) curves and blue (light gray) curves illustrate the data for up-sweep and down-sweep measurements, respectively. These curve shapes include MR jumps near  $B \sim \pm 0.02$  T where the magnetic configuration of Ni electrodes switches from parallel to antiparallel and from antiparallel to parallel. In Fig. 2(a) we observe a positive MR curve at  $V_{SD}=12$  mV, while in Fig. 2(b) we see a small inverse MR curve at  $V_{SD}=15$  mV. At  $V_{SD}=17$  mV [Fig. 2(c)], we get the positive MR feature again. With further increasing  $V_{SD}$ , we get the inverse and positive MR

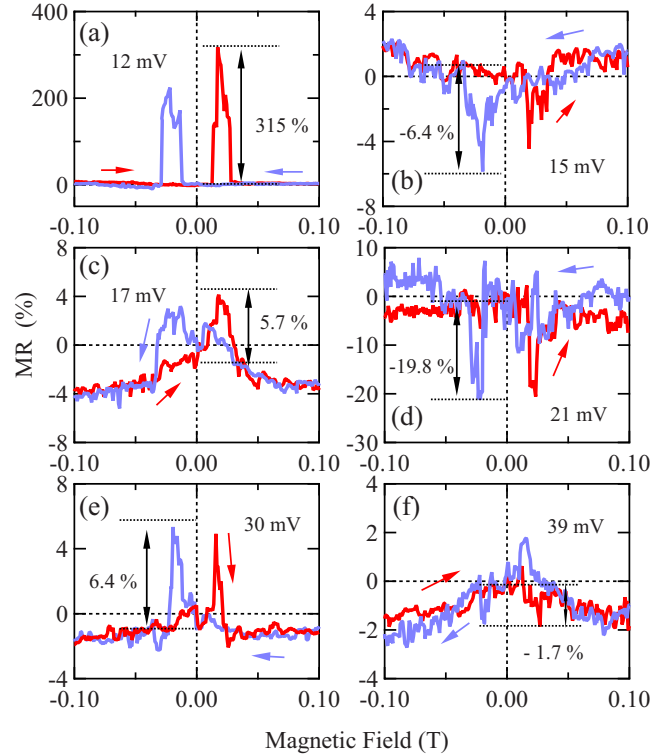


FIG. 2. (Color online) The representative MR curves for various  $V_{SD}$ , (a) 12 mV, (b) 15 mV, (c) 17 mV, (d) 21 mV, (e) 30 mV, and (f) 39 mV, measured at  $V_G=0.1$  V and  $T=50$  mK.

curves continuously in Figs. 2(d)–2(f). It should be noted that the MR curve shape is markedly varied with  $V_{SD}$ . In addition to this, we find an unexpectedly huge MR signal ( $>300\%$ ) in Fig. 2(a). Here, we define the TMR value as the maximum change in the MR value showing hysteretic behavior, as shown in Figs. 2(a)–2(f).

We summarize TMR values as a function of  $V_{SD}$  at  $V_G=0.1$  V in Fig. 3(a). First, an enhanced TMR value is observed in the vicinity of threshold  $V_{SD}$  of the Coulomb blockade.<sup>24</sup> Second, we can clearly see an oscillatory change in the TMR value and the amplitude of the oscillation seems to decay with increasing  $V_{SD}$ . Last, the inverse TMR value observed is relatively small compared to positive TMR one. In Fig. 3(b) we also exhibit the corresponding  $dI/dV_{SD}$ - $V_{SD}$  curve at  $B \sim 0.1$  T. The relatively large  $dI/dV_{SD}$  peaks are seen near 11 and 29 mV, corresponding to the current jumps in Fig. 1(c), and the peak spacing is almost equal to  $E_c$ . The other fine structures derived from the excited states include both positive and negative  $dI/dV_{SD}$  values, as previously described in Fig. 1(c). By a comparison of Figs. 3(a) and 3(b), the  $V_{SD}$  values showing the inverse TMR are qualitatively consistent with those showing the NDC (see arrows). We have confirmed that these tendencies such as the enhanced and inverse TMR values corresponding to the  $I$ - $V_{SD}$  characteristics are reproduced for other Ni/InAs/Ni QDSVs (not shown here). These features are consistent qualitatively with previous theories based on spin accumulation on the QD due to the spin injection.<sup>5,8,9,11–15</sup> Hence, one of the possible origins for our data observed in Fig. 3 is spin accumulation on

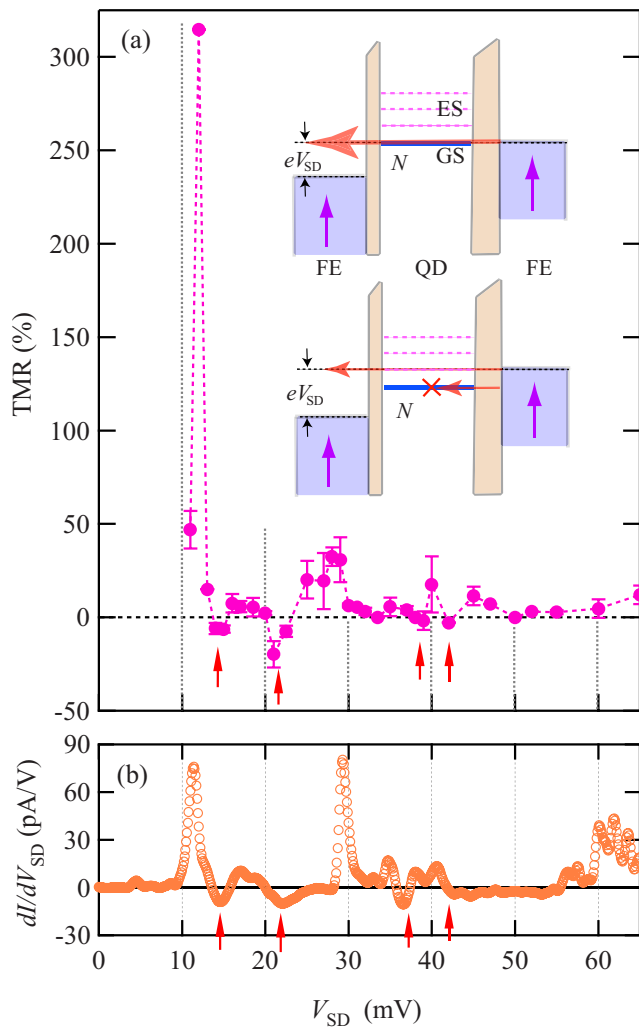


FIG. 3. (Color online) (a) TMR value as a function of  $V_{SD}$  at  $V_G=0.1$  V. The inset shows schematic diagrams of tunneling processes via excited states. An energy window between the occupied and empty states in the right electrodes is opened by applying  $V_{SD}$ . The solid blue and dashed pink lines exhibit the ground and excited states in the QD, respectively. (b) The corresponding  $dI/dV_{SD}-V_{SD}$  curve at  $V_G=0.1$  V and  $B \sim 0.1$  T.

the InAs QD. However, the oscillation period in TMR vs  $V_{SD}$  curves corresponds to the conductance peaks and dips, which result from both the Coulomb staircases and the fine structures shown in Figs. 1(c) and 3(b). With respect to this, since previous theories have reported that the oscillation period corresponds mainly to the Coulomb staircase,<sup>5,8,9,11,13-15</sup> we speculate that our data in Fig. 3 include another influence in addition to the spin accumulation.

Weymann and Barnaś theoretically studied spin-dependent transport properties through a two-level QD weakly and asymmetrically coupled to ferromagnetic electrodes in the sequential tunneling regime,<sup>18</sup> in which their assumption can be somewhat applicable to the present experimental conditions. They theoretically revealed that there is a blocking process of current flows when an electron tunnels to the second level associated with the presence of orbital levels.<sup>18</sup> As shown in Figs. 1(b), 1(c), and 3(b), the

presence of some excited states in the  $I-V$  characteristics can be deduced in our case, so that the current blockade process through the excited states should be involved. The inset of Fig. 3 shows schematic energy diagrams of the tunneling processes of an electron via the ground and/or first excited states. Here, we assume that the eigenstate of the ground state or the first excited state allows mainly up-spin transport or down-spin transport, respectively. When the tunneling of a spin-down electron through the excited state spends a long time in the QD for parallel magnetic configuration because of the minority spin transport, the current flows through the ground state can be blocked (lower diagram), while, when a spin-up electron tunnels through the ground state, the current blockade process can be suppressed because of the majority spin transport (upper diagram). Namely, we can also regard the NDC seen in Fig. 3(b) as a consequence of the tunneling of electrons through the excited states. With varying  $V_{SD}$ , the other transport windows are opened and these consecutive tunneling processes occur through other excited states,<sup>18</sup> so that the TMR can oscillate with ordinary and inverse values.

From these considerations, we now deduce that the observed TMR oscillation results from the above two phenomena: i.e., spin accumulation on the InAs QD and spin-dependent transport properties via excited states in the QD. It seems that not only the presence of the NDC but also the inverse TMR effect is due to the spin accumulation on the QD.<sup>5,8,9,11-15</sup> On the other hand, we also get an inverse TMR effect at  $V_{SD}$  values where the NDC can be seen in the  $I-V$  characteristic, which is consistent with the theory reported by Weymann and Barnaś.<sup>18</sup> To interpret our experimental data, further theoretical studies of spin-dependent transport via excited states including spin accumulation should be required.

Next, we comment on the huge TMR value of  $>300\%$  at  $V_{SD}=12$  mV (around threshold  $V_{SD}$ ). In a previous theory reported by Takahashi and Maekawa,<sup>25</sup> the TMR value in single-electron ferromagnetic transistors can be enhanced by the Coulomb blockade. Yakushiji *et al.*<sup>26</sup> have experimentally demonstrated the enhanced TMR at threshold  $V_{SD}$  of the Coulomb blockade regime. From these facts, it is possible that the TMR value of  $>300\%$  at  $V_{SD}=12$  mV can be affected by the enhanced TMR due to the Coulomb blockade. In our experimental data, spin accumulation on the InAs QD in antiparallel configurations induces slight shifts of the threshold  $V_{SD}$  of the Coulomb blockade.<sup>10</sup> As a consequence, if  $I-V_{SD}$  characteristics have clear Coulomb staircases, as shown in Fig. 1(c), a huge TMR effect can be observed at the threshold  $V_{SD}$ . Second, when we assume Zeeman splitting ( $\Delta E$ ) between spin-up and spin-down states in the InAs QD under a magnetic field and  $V_{SD}$  is smaller than  $\Delta E$ , the QD acts as a spin filter,<sup>27,28</sup> and then highly spin-polarized current can flow from the QD into the ferromagnetic drain electrode through the tunnel barrier. Since we infer that the  $g$  factor of InAs QD is large at least, the above spin-filtering effect can induce the large TMR value in small- $V_{SD}$  regime.

We finally comment on the effect of magneto-Coulomb oscillation, which was discovered by Ono *et al.*,<sup>1</sup> on the transport data described in the present study. In general, the magneto-Coulomb oscillation arises from the exchange splitting at the Fermi level for FEs connected to the island under magnetic fields. This effect can induce resistance changes as

a function of external magnetic field ( $B$ ). Recently, van der Molen *et al.*<sup>29</sup> theoretically claimed that this magneto-Coulomb oscillation is a possible origin of hysteretic MR features for previous carbon-nanotube spin valves.<sup>7</sup> In the Coulomb blockade regime, the conductance ( $G$ ) changes can be expressed by

$$G(q, B) = G(q) + \frac{dG}{dq} \Delta q(B), \quad (1)$$

where  $q$  is the charge state of the island at zero field and  $\Delta q$  is an additional charge. As described in Eq. (1), the conductance is proportional to  $B$  and the conductance increases or decreases *linearly* as a function of magnetic field up to magnetization switching fields. With regard to this, our present data shown in Fig. 2 have almost no linear increase or decrease in the MR with varying magnetic fields before the magnetization switching; MR data change abruptly at the fields where the magnetic configuration of Ni electrodes switches, in particular in Figs. 2(a), 2(d), and 2(e). In addition, the feature seen in Fig. 2(f) including both a positive

MR increase and inverse TMR value cannot be explained only by Eq. (1). These can be considered that the influence of magneto-Coulomb oscillation on the TMR data presented in Fig. 3 is small, but we cannot rule out it completely from the MR data in Fig. 2.

In summary, we have studied TMR effect as a function of  $V_{SD}$  in lateral Ni/InAs/Ni QDSVs showing Coulomb blockade characteristics. With varying  $V_{SD}$ , TMR oscillations can be observed and the oscillation period corresponds to conductance changes observed in  $I$ - $V_{SD}$  characteristics. We also find inverse TMR effect near  $V_{SD}$  values where NDC is observed. A possible mechanism of the TMR oscillation is discussed in terms of spin accumulation on the QD and spin-dependent transport properties via excited states.

K.H. and T.M. thank S. Tarucha, G. E. W. Bauer, A. Oiwa, and A. Cottet for useful discussions. This work is supported by the Special Coordination Funds for Promoting Science and Technology, a Grant-in-Aid from MEXT, Collaborative Research Project of Materials and Structures Laboratory, Tokyo Institute of Technology, and the Sumitomo Foundation.

\*hamaya@iis.u-tokyo.ac.jp

†tmachida@iis.u-tokyo.ac.jp

<sup>1</sup>K. Ono, H. Shimada, S. Kobayashi, and Y. Ootuka, *J. Phys. Soc. Jpn.* **65**, 3449 (1996); K. Ono, H. Shimada, and Y. Ootuka, *ibid.* **66**, 1261 (1997); H. Shimada, K. Ono, and Y. Ootuka, *ibid.* **67**, 2852 (1998).

<sup>2</sup>C. D. Chen, W. Kuo, D. S. Chung, J. H. Shyu, and C. S. Wu, *Phys. Rev. Lett.* **88**, 047004 (2002).

<sup>3</sup>M. M. Deshmukh and D. C. Ralph, *Phys. Rev. Lett.* **89**, 266803 (2002).

<sup>4</sup>A. N. Pasupathy, R. C. Bialczak, J. Martinek, J. E. Grose, L. A. K. Donev, P. L. McEuen, and D. C. Ralph, *Science* **306**, 86 (2004).

<sup>5</sup>K. Yakushiji, F. Ernult, H. Imamura, K. Yamane, S. Mitani, K. Takanashi, S. Takahashi, S. Maekawa, and H. Fujimori, *Nat. Mater.* **4**, 57 (2005).

<sup>6</sup>A. Bernard-Mantel, P. Seneor, N. Lidgi, M. Munoz, V. Cros, S. Fusil, K. Bouzehouane, C. Deranlot, A. Vaures, F. Petroff, and A. Fert, *Appl. Phys. Lett.* **89**, 062502 (2006).

<sup>7</sup>S. Sahoo, T. Kontos, J. Furer, C. Hoffmann, M. Gräber, A. Cottet, and C. Schönenberger, *Nat. Phys.* **1**, 99 (2005).

<sup>8</sup>A. N. Korotkov and V. I. Safarov, *Phys. Rev. B* **59**, 89 (1999).

<sup>9</sup>J. Barnaś and A. Fert, *J. Magn. Magn. Mater.* **192**, L391 (1999).

<sup>10</sup>H. Imamura, S. Takahashi, and S. Maekawa, *Phys. Rev. B* **59**, 6017 (1999).

<sup>11</sup>A. Brataas, Y. V. Nazarov, J. Inoue, and G. E. W. Bauer, *Phys. Rev. B* **59**, 93 (1999).

<sup>12</sup>J. Martinek, J. Barnaś, G. Michalek, B. R. Bulka, and A. Fert, *J. Magn. Magn. Mater.* **207**, L1 (1999).

<sup>13</sup>J. Barnaś, J. Martinek, G. Michalek, B. R. Bulka, and A. Fert, *Phys. Rev. B* **62**, 12363 (2000).

<sup>14</sup>J. Martinek, J. Barnaś, S. Maekawa, H. Schoeller, and G. Schön,

*Phys. Rev. B* **66**, 014402 (2002).

<sup>15</sup>I. Weymann and J. Barnaś, *Phys. Status Solidi B* **236**, 651 (2003).

<sup>16</sup>I. Weymann, J. König, J. Martinek, J. Barnaś, and G. Schön, *Phys. Rev. B* **72**, 115334 (2005).

<sup>17</sup>A. Brataas, M. Hirano, J. Inoue, Y. V. Nazarov, and G. E. W. Bauer, *Jpn. J. Appl. Phys., Part 1* **40**, 2329 (2001).

<sup>18</sup>I. Weymann and J. Barnaś, *J. Phys.: Condens. Matter* **19**, 096208 (2007).

<sup>19</sup>A. Cottet and M.-S. Choi, *Phys. Rev. B* **74**, 235316 (2006).

<sup>20</sup>K. Hamaya, S. Masubuchi, M. Kawamura, T. Machida, M. Jung, K. Shibata, K. Hirakawa, T. Taniyama, S. Ishida, and Y. Arakawa, *Appl. Phys. Lett.* **90**, 053108 (2007).

<sup>21</sup>K. Hamaya, M. Kitabatake, K. Shibata, M. Jung, M. Kawamura, K. Hirakawa, T. Machida, T. Taniyama, S. Ishida, and Y. Arakawa, *Appl. Phys. Lett.* **91**, 022107 (2007).

<sup>22</sup>K. Hamaya, M. Kitabatake, K. Shibata, M. Jung, M. Kawamura, K. Hirakawa, T. Machida, T. Taniyama, S. Ishida, and Y. Arakawa, *Appl. Phys. Lett.* **91**, 232105 (2007).

<sup>23</sup>C. Buizert, A. Oiwa, K. Shibata, K. Hirakawa, and S. Tarucha, *Phys. Rev. Lett.* **99**, 136806 (2007).

<sup>24</sup>The enhanced TMR values of >100% have been observed at around threshold  $V_{SD}$  for other devices.

<sup>25</sup>S. Takahashi and S. Maekawa, *Phys. Rev. Lett.* **80**, 1758 (1998).

<sup>26</sup>K. Yakushiji, S. Mitani, K. Takanashi, S. Takahashi, S. Maekawa, H. Imamura, and H. Fujimori, *Appl. Phys. Lett.* **78**, 515 (2001).

<sup>27</sup>P. Recher, E. V. Sukhorukov, and D. Loss, *Phys. Rev. Lett.* **85**, 1962 (2000).

<sup>28</sup>R. Hanson, L. M. K. Vandersypen, L. H. Willems van Beveren, J. M. Elzerman, I. T. Vink, and L. P. Kouwenhoven, *Phys. Rev. B* **70**, 241304(R) (2004).

<sup>29</sup>S. J. van der Molen, N. Tombros, and B. J. van Wees, *Phys. Rev. B* **73**, 220406(R) (2006).